Calibration of a Chiller Modelica model with experimental data

Christophe Montsarrat¹ Pascal Borel¹ Ana Paez¹

¹EDF R&D, France, firstname.lastname@edf.fr

Abstract

The modelling and calibration of industrial chillers can be challenging, especially when few measurements with a large uncertainty are available. The use of an approximate calibration model is investigated to explore its potential in calibrating a chiller model, constructed in Modelica. Based on the results of a well-instrumented experimental rig of a chiller at the EDF laboratory recorded over five days, with a varying outdoor air temperature, an approximated steady analysis is carried out by calibrating the Modelica model with the experimental results (mass flow rate, temperatures, pressures). The results indicate a good match between the calibrated model and the experiments and a physical sensitivity in the parameters of the model, consistent with the operation of the machine (isentropic efficiency, compressor flow rate, evaporator overheat regulation). Further work can be done on the unsteady measurements recorded on the chiller to improve the model and its stochastic calibration.

Keywords: Chiller modelling, Approximate Bayesian Calibration, Modelica, R507A

1 Introduction

Chillers play a key role in various industries and notably within nuclear power: they enable to condition air that cools down electrical rooms, which are essentials for plant operation and safety. It is thus required to have numerical models that can predict, with required accuracy, the key quantities of these systems, such as the maximum available cooling power under sizing conditions or temperature of the chilled water produced.

Several approaches exist to model these complex systems. A first approach relies on analytical models, often based on a steady-state assumption for the system. It is used to get a quick evaluation of the system behavior, but accuracy is often poor and a large data-set is generally needed to calibrate the model as exhibited by (Cecchinato, Chiarello, and Corradi 2010).

Another model category is the zonal model which consists in establishing a set of equations for each main components of the chiller such as the evaporator, the condenser, the expansion valves and the compressor. Solving the obtained equations systems, either assuming steady state or studying dynamic response, enable to predict the detailed behavior of the system as proposed by (Mouneer, Aly, and Mina 2021), (Afzali and Mahalec 2017) or (Lissandrin et al. 2017).

Computational Fluid Dynamics (CFD) can be used to study the details of the flows within some parts of the chiller. However, this approach is generally not affordable at the integral scale.

Calibration of chiller models is a key aspect of the zonal or analytical as the model relies on parameters that generally cannot be directly deduced from geometry and associated input data of the system. On a design phase, correlations are generally used to compute the required coefficients for the model to run (e.g. heat exchange coefficients). Once the system is in operation, data assimilation techniques can be used to calibrate model parameters. Various techniques can be used to calibrate models: amongst most used methods are least square methods (linear or non-linear), to minimize the differences between observed data and model prediction. In a more general way, Bayesian calibration techniques can be set up to estimate the posterior distribution of the parameters to be calibrated on a given dataset as described by (Marin, Robert, et al. 2007). (Zhen, Niu, and Tian 2023) propose to calibrate a chiller analytical model from the Modelica Buildings library (Wetter et al. 2014) by optimizing the improved indicator of the mean normalized bias error of model predictions.

The primary objective of this study is to calibrate a zonal Modelica chiller model using experimental data obtained from experiments conducted at the EDF laboratory.

First, a description of the Modelica-based chiller models is provided, along with a justification for the approaches used to model the different components of the chiller. Next, the rationale behind the statistical calibration techniques employed is presented, followed by an overview of the experimental facility used for the experiments.

The results from the experiment, considered to be steady, are discussed and then compared with the model predictions resulting from the calibration process. Discussions on the significance of the measurement uncertainties are also addressed.

2 Theory

2.1 Nodal modelling of a chiller

The modelling of a chiller is based on three components developed through an in-house library in Modelica. The motivation is to use components as generic as possible that can be adapted to different configurations of chillers without relying too much on geometric characteristics. As

the motivation is to develop a methodology for calibrating chillers, reducing the number of coefficients for these three main components is essential. The main principles of the components used are quickly presented here:

- **Compressor** - it is modelled by four values: one volumetric flow rate Q_v and three efficiencies quantifying its performance. The three efficiencies quantify the different losses encountered on a compressor: the mechanical efficiency η_{mech} for the friction losses, the volumetric efficiency η_{vol} measuring how efficiently used is the volume sucked in (dead volume, impermeability, pressure loss) and the isentropic efficiency η_{is} quantifying the entropy increase due to the compression of the fluid. These four parameters are important to model the enthalpy increase resulting from the compression rate $\Pi = p_{hp}/p_{lp}$ applied:

$$\Delta h = f(\Pi, Q_v, \eta_{mech}, \eta_{vol}, \eta_{is}) \tag{1}$$

- **Heat exchanger** - the model consists of N discrete cells in which heat exchanges occur between a fluid 1, not changing state, and a fluid 2 that absorbs or releases heat both through sensible exchange and change of state. The exchangers modelled can be parallel or counter flow exchangers, with fluids moving in the same or opposite directions. The cell i-1supplies the inlet conditions for the following cell i(phases, pressure, enthalpy, mass flow rate) and three heat transfer coefficients are used: K_{lat} for the latent heat exchange, $K_{sens,vap}$ and $K_{sens,cond}$, respectively for the sensible exchanges between the vaporized fluid 2 and fluid 1 and the condensed fluid 2 and fluid 1. In the modelling here considered, these three coefficients are kept constant and used as parameters for the calibration. For each cell i, the heat exchange q_i per area units is modelled with the following expression:

$$q_i = K (T_{1,i} - T_{2,i}) \tag{2}$$

The heat flux applied to the cell updates the temperatures at the outlet of the cell i for each fluid (1 and 2) which are then used as the inlet temperatures of the following cell. Depending on the state of the flow (two-phase, vapor or liquid), the coefficients K_{lat} , $K_{sens,vap}$ or $K_{sens,cond}$ respectively apply in (2).

- **Expansion valve** - it is simply modelled by a relationship between the mass flow rate and the pressure difference across the valve. The relationship is the following, with p_{hp} the high-pressure at the inlet and p_{lp} the low pressure at the outlet:

$$\dot{m} = K_{valve} \sqrt{p_{hp} - p_{lp}} \tag{3}$$

A dependency on the coefficient K_{valve} can be added to adjust the opening of the valve, for example using

the overheat, i.e. the temperature difference between the outlet of the evaporator and the saturation temperature within it.

Figure 1 shows a generic chiller model as used in OpenModelica with four main components, representing a classical thermodynamic cycle for a chiller: compression, condensation, expansion and evaporation. The overheat regulation is indicated by the arrow starting at the outlet of the evaporator to regulate the opening of the expansion valve.

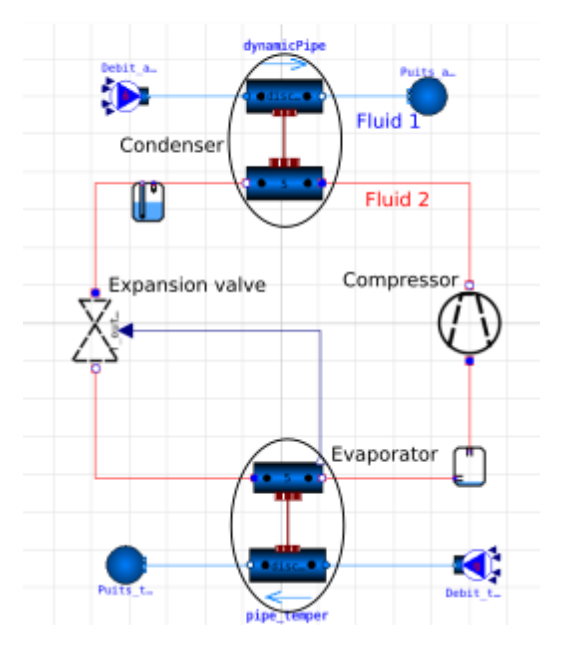


Figure 1. Illustration of a generic chiller model used in the OpenModelica GUI.

2.2 Approximate Bayesian Calibration

The purpose of calibration is to estimate the posterior mutltivariate law of the parameters θ to be calibrated of a model function denoted g. This model, $g(\theta, X)$, predicts observed quantities Y based the parameters to be calibrated and observed input parameters X.

$$Y = g(\theta, X) \tag{4}$$

As implied by the Bayes theorem recalled in Equation 5, the estimation of the posterior distribution of the parameters $\pi(\theta|Y)$ usually requires to be able to express the likelihood $\mathcal L$ of the observed variable Y, given the prediction of the model $\hat Y = g(\theta, X)$.

$$\pi(\theta|Y) = \frac{\mathscr{L}(Y|\theta)\pi(\theta)}{\pi(Y)} \tag{5}$$

A usual approach is to assume that the discrepancies between model prediction \hat{Y} and the measured variable Y,

denoted ε , follow a multivariate gaussian law with a null mean. If the errors are homoscedastic, non correlated and the model $g(\theta, X)$ is linear or locally linear using Taylor expansion, one can apply the Gauss-Markov theorem to obtain the ordinary least square (OLS) estimator $\hat{\theta}$ and its associated variance covariance matrix Σ . Assuming the likelihood function $\mathcal{L}(Y|\theta)$ is Gaussian, the posterior distribution can be expressed as:

$$\pi(\theta|Y) = \mathcal{N}(\hat{\theta}, \Sigma)$$
 (6)

In both linear and nonlinear Gaussian calibration approaches, it is further assumed that the prior distribution $\pi(\theta)$ is multivariate Gaussian. These methods rely on the Gaussian nature of the likelihood and require that the residuals—i.e., the differences between model predictions and observations—have zero mean. This implies that discrepancies are attributed solely to measurement uncertainties, rather than model bias or structural errors.

When the likelihood $\mathcal{L}(Y|\theta)$ has no analytical form, a solution is to use likelihood-free techniques such as the approximate bayesian calibration (ABC method), as suggested by (Turner and Zandt 2012) or (Cant and Evins 2023). This method mainly rely on the definition of a metrics to compare the simulated quantities \hat{Y} to the same observed quantities Y. A threshold ε_0 is then associated to this metrics to consider a candidate point θ producing calibrated quantities. This is equivalent to considering that if the candidate point $\hat{\theta}$ produces predictions close enough to the observed values, then this point has a nonzero probability of being in the posterior parameter distribution $\pi(\theta|Y)$ as illustrated in Equation 7.

$$\pi(\theta|Y) \approx \pi(\theta|\rho(\hat{Y},Y) \le \varepsilon_0)$$
 (7)

This approach can also accommodate the presence of model error by specifying a probability density function f_{ε} to represent it. Using a fixed acceptance threshold, as described above, is equivalent to assuming that the model error follows a uniform distribution. In this case, all discrepancies within the threshold are considered equally likely, regardless of their magnitude. A common metrics used is the sum of the squared errors between the predictions and the observations.

$$RMSE_{Y_i} = \sqrt{\frac{1}{n_{obs}}} \sum_{observation} (Y_i^{pred} - Y_i^{obs})^2$$
(8)

$$MBE_{Y_i} = \frac{1}{n_{obs}} \sum_{observation} (Y_i^{pred} - Y_i^{obs})$$
(9)

$$CvRMSE_{Y_i} = \frac{RMSE_{Y_i}}{\overline{Y_{obs}} - Y_{ref}}$$
(10)

$$MBE_{Y_i} = \frac{1}{n_{obs}} \sum_{observation} (Y_i^{pred} - Y_i^{obs})$$
 (9)

$$CvRMSE_{Y_i} = \frac{RMSE_{Y_i}}{\overline{Y_{obs}} - Y_{ref}}$$
 (10)

$$NMBE_{Y_i} = \frac{MBE_{Y_i}}{\overline{Y_{obs}} - Y_{ref}} \tag{11}$$

Common threshold to retain a candidate point is to have $CvRMSE \le 0.2$ and $NMBE \le 0.05$ for each observed variable.

Using OpenTURNS (Baudin et al. 2017), a candidate set sample is generated from the multivariate distribution $\pi(\theta)$. Then, for each candidate point, the model g is evaluated allowing the defined metrics to be computed. The multivariate law of the posterior sample is then inferred using parametric or non parametric methods to define notable the most probable posterior values of $\pi(\theta|Y)$. If the posterior sample does not contain enough points regarding a targeted size previously defined, additional samples from the prior distributions can be considered. The above presented algorithm is usually called the basic ABC-rejection algorithm which can be improved using sequential MonteCarlo approach.

3 The R507 Chiller Experiment

Global Description 3.1

The test facility (Figure 2) used in this study operates with R507A, a hydrofluorocarbon (HFC) refrigerant (CoolProp n.d.). The test facility is well-equipped with pressure and temperature sensors installed at the inlet and outlet of each component, complemented by several Coriolis flow meters integrated into the test facility system.

The test facility consists of three main circuits. The first circuit, using Temper 55 as the secondary fluid in the evaporator, is designed to measure the cooling demand. This circuit includes electrical resistances and a pump that allow for the control of flow rate, temperature, and thermal power dissipation. A second air circuit interacts with the condenser to dissipate heat from the refrigerant. The third circuit utilizes R507A as the working fluid and forms the core of the experimental setup.

The refrigeration system consists primarily of a plate evaporator with a surface area of 44.4 m², a condenser of 1157.5 m² equipped with five variable-speed fans, an electronic expansion valve, and a Grasso rotary screw compressor. The compressor allows for variations in the internal swept volume. Depending on the applied compression ratio, the refrigerant flow rate can range from 23.1 m³/h to $231 \,\mathrm{m}^3/\mathrm{h}$.



Figure 2. Photo of the test facility

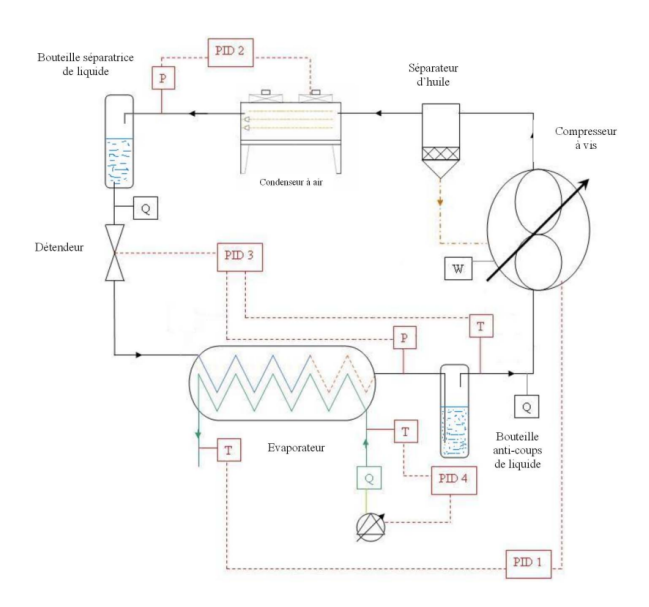


Figure 3. Experimental setup with control loop

Figure 3 shows the four controllers (PID1, PID2, PID3, and PID4) used to regulate the precision of the evaporator, high pressure, overheating, and the secondary pump flow rate of the evaporator circuit, respectively. These regulations will not be considered in the current model.

3.2 Uncertainty of measurements

The expanded uncertainty of each sensor considers the whole measuring chain, from the sensor to the automate errors. The uncertainty given corresponds to a confidence interval of 95%.

The mass flow rate, pressure, and temperature sensors have an accuracy at $\pm 0.1\%$, $\pm 3\%$, and $\pm 0.174^{\circ}$ C, respectively. It must however be noted that the uncertainties on the measurements on the air-side of the condenser are higher and more difficult to estimate.

When a calculation includes several variables, for example the calculation of the cooling capacity, a combined standard uncertainty U_c^2 should be calculated using the equation 12. The method is based on first-order Taylor series, and it is referred to as the law of propagation of uncertainty (Taylor, Barry N and Kuyatt 1994).

$$U_c^2(y) = \sum_{i=1}^n \left(\frac{\partial f}{\partial x_i}\right)^2 u^2(x_i) + \sum_i \sum_j \partial_i f \partial_j f r_{ij} u_i u_j \quad (12)$$

where $u(x_i)$ represents the uncertainty of each variable. In this article, the variables are assumed to be independent and with a linear behavior, which allows to neglect the last term of the previous equation that refers to the correlation between the variables.

3.3 Experimental conditions

The experimental results presented in this study were obtained under the following conditions:

- The flow rate of the Temper-55 fluid was maintained at 6 kg/s using the circuit pump. The evaporator pressure was kept constant at 7.5 bar through compressor regulation. To simulate a cooling demand, electrical resistances installed in the Temper-55 circuit provided a constant thermal load of 100 kW.
- The refrigerant overheat was regulated by the expansion valve, ensuring a stable overheat of 6°C. The five fans of the air-condenser operated continuously at maximum speed, allowing the refrigerant's high pressure to vary according to the ambient air temperature.
- Data were recorded every 10 seconds over a period of five days.

4 Results and discussions

4.1 Experimental results

The analysis of the results revealed significant oscillations primarily due to the ambient air temperature and the simultaneous regulation of four controllers, see section 3.1. While these oscillations could provide valuable insights in a future phase, particularly when incorporating regulation into our models for dynamic comparisons with experimental data, our current study focuses on a steady-state analysis.

In order to validate and calibrate the models in steadystate conditions, the experimental results were divided into multiple intervals where the ambient temperature variation remained below 1°C.

Figure 4 illustrates the fluctuations of air temperature during the recording test. To ensure a clear and reliable validation of the model, four representative points are selected on the following criterion: the temperature remains in a $\pm 1^{\circ} C$ range for at least one hour. The different variables measured and their mean values over these intervals are presented in Table 1.

To validate the data collected from the test facility, an energy balance was performed for both the evaporator, (13) and the global system (14). The energy balance in the condenser was not calculated due to the imprecision of the air measurements.

$$\dot{m}_{\text{Temper}} c_{p\text{Temper}} \Delta T_{\text{Temper_evap}} = \dot{m}_{\text{R507A}} \Delta h_{\text{R507A_evap}}$$
(13)

$$\dot{Q}_{\text{evan}} + \dot{Q}_{\text{cp}} = \dot{Q}_{\text{cond}} \tag{14}$$

Figure 5 shows the statistical variations in thermal capacity and the energy balance results for point 0. The data is presented using box plots, as this format allows for the display of key information in a single figure, such as the mean and distribution data. The black boxes represent the data distribution, with the blue horizontal lines inside indicating the mean and the red lines representing the median.

| Point | T_air (°C) | Q_R507A (kg/s) | HP (bar) | BP (bar) | T_evap,out (°C) | T_comp,out (°C) | T_cond,out (°C) |
|-------|------------|----------------|----------|----------|-----------------|-----------------|-----------------|
| 0 | 19.06 | 0.841 | 12.32 | 7.55 | 11.09 | 48.20 | 20.82 |
| 1 | 16.50 | 0.828 | 11.88 | 7.55 | 10.88 | 48.43 | 19.30 |
| 2 | 15.42 | 0.815 | 11.43 | 7.54 | 10.69 | 48.31 | 17.82 |
| 3 | 19.89 | 0.847 | 12.72 | 7.56 | 11.06 | 48.37 | 22.03 |

Table 1. Experimental results under different steady-state conditions

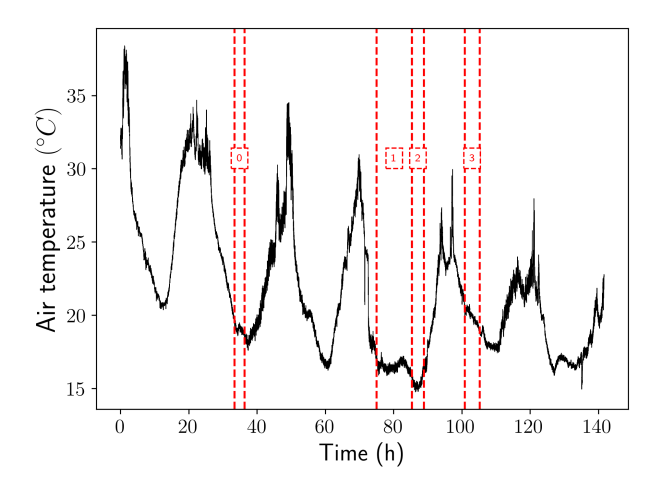


Figure 4. Evolution of the air temperature, measured at the air condenser. The four experimental periods corresponding to the four approximate steady conditions are indicated by the red dashed lines.

The ends of the boxes denote the first and third quartiles, while the black "whiskers" extend to the minimum and maximum values.

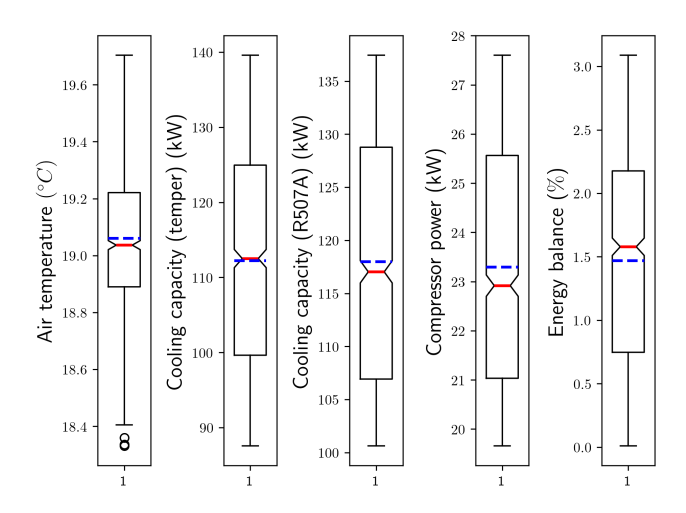


Figure 5. Box plot at point 0 comparing the thermal power exchanged at the evaporator and condenser. Energy balance of the system. Median: red bar, Mean: blue line.

The energy balance revealed a small discrepancy, less than 2.5~%, which validates the measurements taken in the test facility.

4.2 R507 model and calibration

4.2.1 Presentation of the R507 model

A Modelica model has been used to capture the behaviour of the chiller tested experimentally. As explained in 3.3, the aim is to model steady-like behaviors of the system. The assumption here made considers that the air temperature fluctuations are small enough to approximate the operations of points 0 to 3 to steady conditions. The chiller is modelled with four main components as shown in Figure 1 and presented in 2.1. Here, the different parameters to be calibrated are presented along with the setup used in OpenModelica.

Most of the modelling is based on an adapted version of the Modelica Standard Libry (MSL) except for the types of fluid used in the model. Indeed, the MSL does not integrate the possibility of utilising fluids like R507A and Temper-55. The two fluids can be introduced by using the open source library CoolProp (Bell et al. 2014), whose integration into the software OpenModelica has been done with the library ExternalMedia (Casella and Richter 2008).

Overall, twelve uncertainties and parameters can be calibrated in the model as shown in Table 3. They correspond to the uncertainties associated to the values measured experimentally and to the parameters of the components of the model (heat exchange coefficients, efficiency, overheating). The way they are calibrated is explained in the next section based on the methodology described in 2.2. Large uncertainties for the air temperature and mass flow rates were initially taken in the a priori distributions (2°C and 1 kg/s resp.): the resulting calibrated point is consistent with this choice.

The prior distributions are chosen based on the knowledge of the uncertainties (U) and the parameters. For the uncertainties, the value is sampled into a normal distribution centred into 0 and with a standard deviation corresponding to the uncertainty of the probe (temperature or mass flow rate). This is added to the observed value experimentally as an input of the model. Regarding the rest of the parameters, their distribution is chosen uniform with bounds determined as much as possible from the experience of the user: the larger is the range, the more unphysical operating points for the model will be computed, leading to important errors between the model and the experiment or simply difficulties for the model to converge.

4.2.2 Calibration

Given a random sampling of all the uncertainties of measurements and the parameters to be calibrated in the model done *N* times according to prior distributions of probability, the principle of the ABC method is to compare the values obtained with the model to the experiment and then select the most relevant.

| Min C _v RMSE | $\operatorname{Min} C_{v}RMSE$ | Min NMBE | Max NMBE |
|-------------------------|--------------------------------|----------|----------|
| 0 | 0.2 | -0.2 | 0.2 |

Table 2. Range of acceptable errors for the selection of the parameters of the model.

The relevance is based on criteria defined by the user depending on the values observed and the tolerance accepted for the calibration in terms, for example, of the mean bias error (MBE) and the root mean square error (RMSE) with the experimental measurements. These two criteria are the ones retained for the selection of the points in the sample and can be written as follows for each value observed, as explained in 2.2.

The ranges for the selection of the parameters are indicated in Table 2. It means that, for one set of parameters from the sample, when comparing the values obtained with the model, the set is conserved if the RMSE and MBE are in the range indicated. The choice of 20% enables to keep sets of parameters with a reasonable error compared to the experiment.

The size of the design of experiments concerns 5000 simulations of approximately 30 seconds CPU, that have been carried out. With the RMSE and MBE criteria below 20%, only 6 of them have been selected. By making the criteria looser, for example with accepting results with a 30% error on the RMSE and MBE, 127 could have been retained. Here, the motivation was to show the principle of the method and the good possibilities for a calibration but this could be improved to get a larger sample for the posterior distributions. Also, out of the 5000 samples, some lead to unphysical behaviors and never converge in the model. These can be kept and analyzed to actually understand the potential problems of robustness of the model to the parameters. Only fifty out of the 5000 samples failed in this case, indicating quite a robust model, numerically.

The optimal point for the different parameters and uncertainties calibrated is shown in Table 3. These are determined with the resulting distributions built on the selected points of each parameter. The most probable value in each distribution obtained corresponds to the optimal value.

Figures 6 and 7 show the distributions of the isentropic effiency η_{is} and Q_{ν} , prior and posterior to the approximate bayesian calibration. The distribution in green represents the distribution on which the parameters are drawn to simulate the behaviour of the chiller with the model and the orange one represents the points for which the selection criteria are fulfilled. The blue curve gives an approximation of the orange distribution based on a kernel smoothing

| $U_{T_{air}}$ | $U_{Q_{air}}$ | $U_{T_{temper}}$ | $U_{Q_{temper}}$ | K_{lat}^{cond} | K_{sg}^{cond} |
|-----------------|------------------|------------------|----------------------|------------------------|-----------------|
| -1.61 °C | $-0.78 \ kg/s$ | -0.14 °C | $-0.32 \ kg/s$ | 160.9 | 136 |
| K_{sl}^{cond} | K_{lat}^{evap} | K_s^{evap} | $Q_{v}^{compressor}$ | $\Delta T_{valve,nom}$ | η_{is} |
| 140.8 | 134.5 | 117.9 | $0.022 m^3/s$ | 5.26 °C | 0.398 |

Table 3. Table of the optimal values based on the calibration done with the R507 model.

| Q_{R507} | Pcond | p_{evap} | |
|---------------------------|---------------------------|----------------------------|--|
| Mass flow rate of R507 | Pressure in the condenser | Pressure in the evaporator | |
| T _{out,evap} | $T_{in,cond}$ | T _{out,cond} | |
| Temperature at the outlet | Temperature at the inlet | Temperature at the outlet | |
| of the evaporator | of the condenser | of the condenser | |
| $P_{th,evap}$ | | | |
| Thermal power exchanged | | | |
| at the evaporator | | | |

Table 4. Description of the observed measurements used for the comparison with the model.

method (Baudin et al. 2017). A peak in the distribution can be noticed in both cases, meaning that the model is very sensitive to these two parameters for the calibration. Given a compression ratio, the temperature at the inlet of the condenser is strongly affected by the isentropic efficiency. Being too far from $\eta_{is}=0.398$ therefore seems to lead to probable large errors on the calibration. The same can be inferred on Q_v , which controls the mass flow of the refrigerant. For three other parameters, the posterior distribution is quite different from the prior choice, which indicates a sensitivity of the model to these parameters to be consistent with the experimental observations (ΔT_{valve} , $U_{T_{air}}$ and K_s^{evap}).

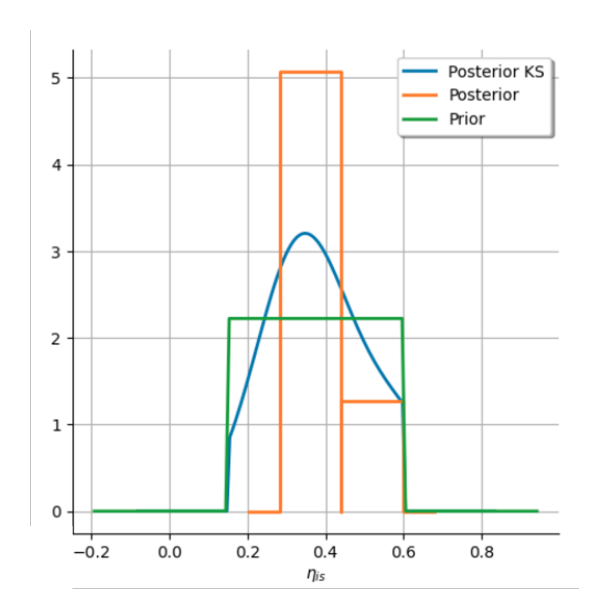


Figure 6. Distribution of the isentropic efficiency, prior and posterior to the application of the ABC method and the selection. The blue distribution approximates the distribution of orange values selected with a kernel smoothing.

It is now interesting to compare the predictions of the model with the optimal set of parameters determined with the ABC method to the actual observations measured experimentally as described in Table 4.

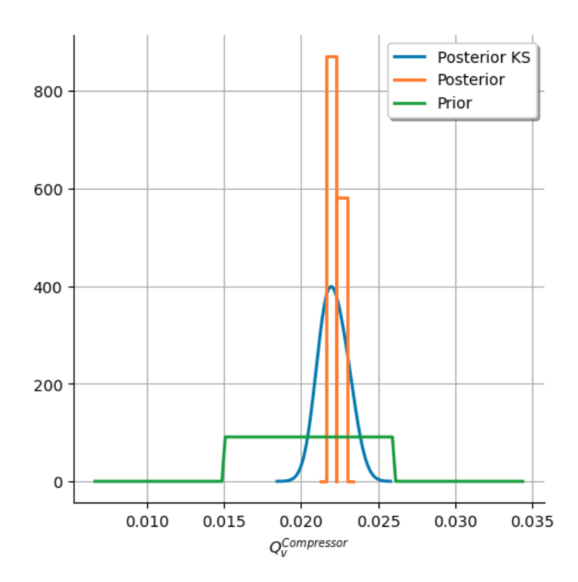


Figure 7. Distribution of the compressor volumetric flow, prior and posterior to the application of the ABC method and the selection. The blue distribution approximates the distribution of orange values selected with a kernel smoothing.

Figure 8 compares the predictions from the model with the experimental values measured on the mass flow rate of refrigerant. The blue dots show the initial predictions based on the most probable set of parameters with the prior distributions whilst the orange dots indicate the predictions from the posterior, built distributions from the selection. The green line is the first bisector corresponding to a perfect equality between predictions from the model and experiments for the different observations. Overall, the ABC method leads to a good calibration of the model, improving clearly the match between experiment and modelled results.

Another view on the comparison between the experiment and the model is shown in Figure 9. It compares the cycles for point 0 (cf. Table 1). What can be observed is the overestimate of the pressure at the condenser for four sets of parameters. The fifth set corresponds to the optimal point and matches quite well with the experimental cycle. Other differences concern the enthalpy at the outlet of the condenser (slight difference) and the specific enthalpy at the compressor outlet.

The advantages of the ABC calibration method over more traditional approaches are clearly demonstrated in this case. Due to the complexity of the model, certain parameter evaluations may lead to simulation failures—situations that ABC is uniquely equipped to handle, as it does not require explicit likelihood evaluations. As illustrated in Figure 6 and Figure 7, the resulting posterior distributions are approximately Gaussian. ABC enables the generation of a discrete sample from this posterior, providing a flexible and robust inference framework. Given the typically nonlinear nature of the models, conventional methods such as nonlinear least squares or nonlinear Gaussian calibration often suffer from poor explo-

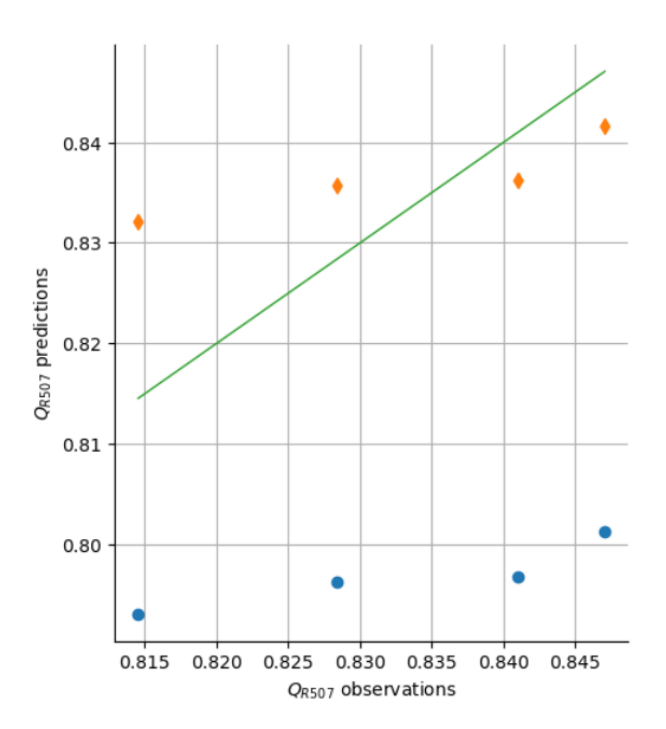


Figure 8. Distribution of the compressor volumetric flow, prior and posterior to the application of the ABC method and the selection. The blue distribution approximates the distribution of orange values selected with a kernel smoothing.

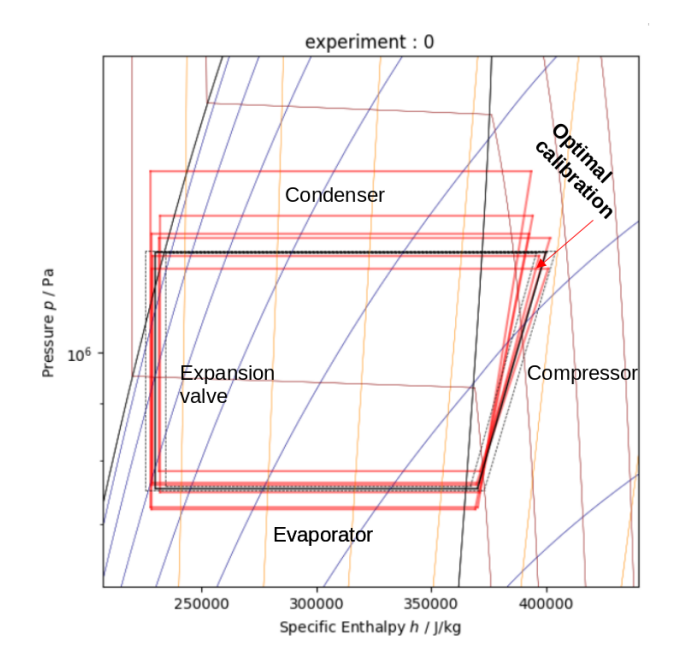


Figure 9. Representation of the experimental cycle for point 0 (black lines) and the ones obtained with the model after calibration with the ABC method. The point resulting from the optimum values in the calibration is shown by the arrow.

ration of the parameter space and high sensitivity to initial conditions. In contrast, ABC facilitates a more comprehensive exploration, especially when the likelihood is intractable or the model is prone to numerical instabilities. Moreover, due to limited prior knowledge about the model parameters, a uniform prior distribution is often the most

appropriate choice. Gaussian priors, by contrast, may introduce unwarranted assumptions and overly constrain the calibration process.

Generally, the calibration enables a quite satisfying fit of the model with the experiment for the four observations on the different values. Although a larger shift can be observed for the inlet temperature at the condenser (or outlet temperature of the compressor), the overall prediction is improved with the calibration. That shift could be explained by the choice made for modelling the compressor with constant efficiencies: a variation of the volumetric and isentropic efficiencies with the pressure ratio may improve these results (Gicquel 2001).

5 Conclusions and further work

This study was motivated by the use of an approximate calibration method for the modelling of a chiller. To the knowledge of the authors, this kind of methods for this type of applications has rarely been done before. Experimental results on a chiller test facility at EDF have been obtained and used to make a calibration of a model representing the chiller in *Modelica*.

With four experimental points approximated as being in a steady state, a calibration has been performed based on the approximate bayesian calibration method. Considering seven variables observed experimentally for these four points, a set of parameters is varied in the model following a design of experiments constructed on probabilistic distributions a priori. The calibration done has consisted in selecting the sets of parameters ensuring an acceptable error between the experiments and the variables modelled.

The results obtained with the calibration are satisfying as they enable to maintain the error below 20% for the sets of parameters kept. Given the initial number of parameters in the model, the ABC method also offers a very interesting way of priorizing the parameters regarding the sensitivity of the variables of interest in the model. In our case, consistently with what is physically modelled, the isentropic efficiency, the volumetric flow rate and the nominal overheating for the expansion valve are the most sensitive parameters.

It is interesting to comment on the use of such methods to analyze further experimental results. In this study, the choice was to start with approximating steady regimes for the chiller with the experimental results based on an assumption of low variations of the outdoor air temperature. The analysis here presented shows that it is possible to calibrate the model to these experimental conditions but it also shows that only a few points are kept in the end, out of the 5000 samples. Different improvements to the current application of the method can be listed here for further work:

Treating the problem as an unsteady one by considering the variations of the variables over time. In practice, it means that for each time step in the sample considered, the variables observed correspond to an

experimental point and the same method can be used with more experimental points. This would imply an improvement of the model to account for the regulation loops in the experiment but also an increase in the CPU cost, with more observations in the method.

- Improving the components of the model: the compressor efficiencies depend on the pressure ratio, which is not the case in the current model. Also, the air-cooled condenser is modelled with a counterflow heat exchanger whilst in reality, it is a cross-flow exchanger.
- With more points selected for the probabilistic distributions, it would then be interesting to transpose the posterior distributions to more extreme air temperature conditions, beyond 40°C, to make an evaluation of the uncertainties, in particular on the cooling power of the chiller.
- The choice of the prior distributions is essential to avoid non-physical and unstable numerical points in the model. A careful investigation of that choice can significantly help the process of calibration.

Acknowledgements

This work has been supported by Electricité de France (EDF) and the collaboration of three departments: MFEE (Fluid Mechanics, Energy and Environment), TREE (Technologies and Research for Energy Efficiency) and PRISME (Performance, Industrial Risk and Monitoring for Maintenance and Operation).

References

Afzali, Sayyed Faridoddin and Vladimir Mahalec (2017). "Optimal design, operation and analytical criteria for determining optimal operating modes of a CCHP with fired HRSG, boiler, electric chiller and absorption chiller". In: *Energy* 139, pp. 1052–1065. ISSN: 0360-5442. DOI: https://doi.org/10.1016/j.energy.2017.08.029. URL: https://www.sciencedirect.com/science/article/pii/S0360544217314056.

Baudin, Michaël et al. (2017). "Openturns: An industrial software for uncertainty quantification in simulation". In: *Handbook of uncertainty quantification*. Springer, pp. 2001–2038.

Bell, I. et al. (2014). "Pure and Pseudo-pure Fluid Thermophysical Property Evaluation and the Open-Source Thermophysical Property Library CoolProp". In: *Industrial Engineering Chemistry Research*. URL: https://pubs.acs.org/doi/full/10.1021/ie4033999.

Cant, Kevin and Ralph Evins (2023). "Improved calibration of building models using approximate Bayesian calibration and neural networks". In: *Journal of Building Performance Simulation* 16.3. Publisher: Taylor & Francis _eprint: https://doi.org/10.1080/19401493.2022.2137236, pp. 291–307. DOI: 10.1080/19401493.2022.2137236. URL: https://doi.org/10.1080/19401493.2022.2137236.

Casella, F. and C. Richter (2008). "ExternalMedia: a Library for Easy Re-use of External Fluid Property code in Modelica". In: *The Modelica Association*.

- Cecchinato, Luca, Manuel Chiarello, and Marco Corradi (2010). "A simplified method to evaluate the seasonal energy performance of water chillers". In: *International Journal of Thermal Sciences* 49.9, pp. 1776–1786. ISSN: 1290-0729. DOI: https://doi.org/10.1016/j.ijthermalsci.2010.04.010. URL: https://www.sciencedirect.com/science/article/pii/S1290072910001092.
- CoolProp (n.d.). "R507A defined in Coolprop". In: (). URL: https://coolprop.org/fluid_properties/fluids/R507A.html.
- Gicquel, Renaud (2001). *Compresseurs volumétriques*. Vol. Systèmes énergétiques, tome 1. Mines de Paris.
- Lissandrin, Marco et al. (2017). "Optimal operational efficiency of chillers using oil-free centrifugal compressors". In: *International Journal of Refrigeration* 82, pp. 83–96. ISSN: 0140-7007. DOI: https://doi.org/10.1016/j.ijrefrig.2017.05.019. URL: https://www.sciencedirect.com/science/article/pii/S0140700717302104.
- Marin, Jean-Michel, Christian P Robert, et al. (2007). *Bayesian core: a practical approach to computational Bayesian statistics*. Vol. 268. Springer.
- Mouneer, Tarek A., Mohamed H. Aly, and Ehab M. Mina (2021). "Optimal design configuration and operating sequencing of hybrid chiller plant: A case study of hotel building in Cairo, Egypt". In: *Journal of Building Engineering* 42, p. 102796. ISSN: 2352-7102. DOI: https://doi.org/10.1016/j.jobe.2021.102796. URL: https://www.sciencedirect.com/science/article/pii/S2352710221006549.
- Taylor, Barry N and Chris E Kuyatt (1994). "NIST Technical Note 1297 Guidelines for Evaluating and Expressing the Uncertainty of NIST Measurement Results". In: *Technology*.
- Turner, Brandon M. and Trisha Van Zandt (2012). "A tutorial on approximate Bayesian computation". In: *Journal of Mathematical Psychology* 56.2, pp. 69–85. ISSN: 0022-2496. DOI: https://doi.org/10.1016/j.jmp.2012.02.005. URL: https://www.sciencedirect.com/science/article/pii/S0022249612000272.
- Wetter, Michael et al. (2014). "Modelica Buildings library". In: *Journal of Building Performance Simulation* 7.4, pp. 253–270. DOI: 10.1080/19401493.2013.765506. URL: https://doi.org/10.1080/19401493.2013.765506.
- Zhen, Cheng, Jide Niu, and Zhe Tian (2023). "Research on Model Calibration Method of Chiller Plants Based on Error Reverse Correction with Limited Data". In: *Energies* 16.2. ISSN: 1996-1073. DOI: 10.3390/en16020918. URL: https://www.mdpi.com/1996-1073/16/2/918.